

Fragility based damage assesment in existing precast industrial buildings: A case study for Turkey

Sevket Murat Senel[†] and Ali Haydar Kayhan

Department of Civil Engineering, Pamukkale University, Kinikli Kampusu, Denizli, Turkey

(Received May 12, 2009, Accepted October 7, 2009)

Abstract. In Turkey, majority of industrial facilities are composed of precast buildings. However, precast buildings have suffered extensive damage during Kocaeli and Duzce (1999) and Adana-Ceyhan (1998) earthquakes. Therefore, in this study, fragilities of existing building stock and damage probabilities of precast buildings were studied. For this purpose, building inventories were prepared and variation of structural parameters was determined by investigating the design project of 65 precast buildings constructed in Denizli, Turkey. Twelve analysis models which reflect the stiffness, strength and ductility properties of building inventory were constructed. After the definition of strain based displacement limits and corresponding damage states for buildings, displacement demands were calculated by using non linear time history analysis. During the analyses 360 strong ground motion records were used. Exceedence ratios of concerned damage limits was calculated by checking the displacement demands and then PGV based fragility curves were constructed. Efficiency of strength, stiffness and ductility properties of existing precast buildings were investigated by comparing the fragility curves. The results have shown that the most effective parameters that govern the damage probabilities of precast buildings are stiffness and ductility. It was also stated that the results of fragility analysis and damage and failure observations performed after Kocaeli and Duzce Earthquakes are compatible.

Keywords: precast industrial buildings; fragility curves; strain based damage; damage states; damage estimation; nonlinear analysis.

1. Introduction

Especially since 1980's, there has been a great demand to industrial facilities due to increasing private investments. It is reported that approximately 90% of lightweight industrial facilities were constructed by using precast members (Karaesmen 2001). Short duration of construction period, respectively low investment prices due to prefabrication, higher allowance for quality control and capability of higher workmanship and material quality are some advantages for the use of precast buildings. As opposed to their advantages, precast industrial buildings have suffered excessive damage during strong earthquakes occurred especially in last two decades in Turkey. Site investigations performed after Adana-Ceyhan (1998) and Kocaeli and Duzce earthquakes (1999) which hit the home of important industrial lands of Turkey have shown that seismic performances of precast industrial buildings are inadequate.

[†] Assistant Professor, Ph.D., Corresponding author, E-mail: smsenel@pau.edu.tr

According to building inventories prepared after Kocaeli Earthquake, direct or indirect economic losses due to damage were reported in approximately 60% of industrial facilities (Cruz and Steinberg 2005). In Turkey, 98% of industrial lands are located in seismically active regions (Adalier and Aydingun 2001) and aforementioned losses clearly indicate that industrial regions greatly composed by precast buildings are under same risk.

Site investigations and theoretical studies performed by different researchers explained the weak points of precast buildings by means of inadequate stiffness and strength and/or problems caused by insufficient connection details (Arslan *et al.* 2005, Saatcioglu *et al.* 2001, Zorbozan *et al.* 1998). In this study, damages associated with the connection details and problems were not taken into consideration. Among these problems, large displacement demand caused by inadequate stiffness was especially emphasized by various researchers (Atakoy 2000, Posada and Wood 2002). Lower strength levels considered in design with respect to Eurocode 8 (1998) and Uniform Building Code (UBC-1997) was the another point associated with the damage in precast buildings (Arslan *et al.* 2005, Tezcan and Colakoglu 2003). The number of studies which explain the reasons behind the excessive damage can be increased. Although Adana-Ceyhan and Kocaeli-Duzce regions are quite far from each other (Fig. 1), structural properties and observed damage types of precast buildings are very similar. This situation implies that the problems related with precast industrial structures are not site specific, but wider and common.

The wider and common damage has emphasized the need for risk assessment in able to estimate potential damage for future earthquakes. For this purpose, fragility curves which allow the estimation of damage probabilities as a function of ground motion indices (PGA, PGV) or structural parameters (S_d) are utilized as useful tools. The results of fragility analysis can be used for damage and loss estimation and disaster response planning studies (Kirçil and Polat 2006). Fragilities associated with the damage probabilities can also be evaluated as the indicator of efficiency of structural parameters considered or compared.

In this study, fragility curves are used to make risk assessment of existing precast buildings and to

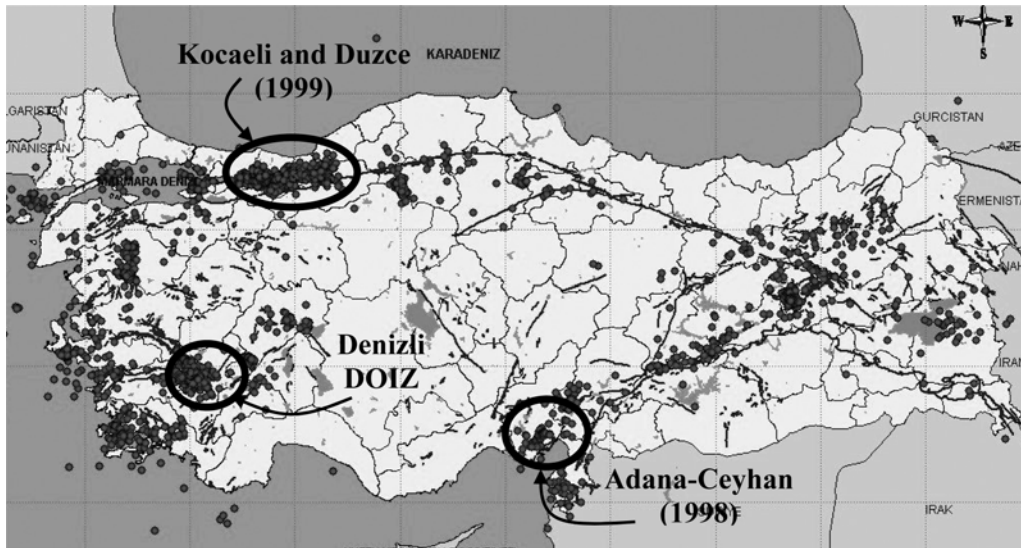


Fig. 1 Regions suffered from precast building damages in recent earthquakes and location of DOIZ

investigate the efficiency of structural parameters determined during inventory study. Precast industrial building inventories were obtained by investigating the design projects of buildings constructed in Denizli Organized Industrial Zone (DOIZ). Denizli city is located in high seismicity Aegean region of western Turkey as shown in Fig. 1. Typical building models were prepared by using the structural properties obtained from the inventory and by considering the previous studies based on damaged buildings. SDOF systems which represent the strength, stiffness and ductility properties of building models were constructed and displacement demands were calculated by using non-linear time history analyses. During the time history analysis, 360 strong ground motion records which are classified according to PGV values were used. Damage assessments of structural models were performed by using strain based damage limits and then PGV based fragility curves were constructed by using lognormal distribution. Consequently, efficiency of structural parameters (strength, stiffness and ductility) on damage probability was determined. Under the light of these findings the damage risk in existing precast buildings and the efficiency of code definitions were discussed.

2. Typical properties of precast industrial buildings

There are a lot of studies in the literature performed after Adana-Ceyhan (1998) and Kocaeli and Duzce (1999) Earthquakes that explain the structural properties of precast buildings. In these studies structural forms, typical bay widths, member and section dimensions, material properties were investigated (Sezen *et al.* 2000, Posada and Wood 2002, Sezen and Whittaker 2006) and the relation between these properties and the structural damages were discussed. On the other hand, it can be said that the reported properties were generally collected from the damaged buildings and therefore does not represent the general view that also includes the undamaged ones. While collecting the building inventories this situation was taken into consideration and precast buildings were selected from another high seismicity region which was not tested with strong earthquakes yet. Affected regions in Kocaeli and Adana-Ceyhan Earthquakes and Denizli city where the building inventories collected are sketched on representative seismic intensity map as shown in Fig. 1. Building Inventory was prepared by using the design projects of 65 precast industrial buildings. Structural properties such as building and member dimensions, material properties, transverse and longitudinal reinforcement ratios were determined and statistical variation of these parameters were investigated.

In order to make visualization of the problem, typical configuration of precast industrial buildings, which represents the large proportion of Turkish industrial building stock and therefore considered in this study, is shown in Fig. 2. The frames compose of cantilever columns connected with roof girders in transverse direction and gutter beams and purlins in longitudinal direction. Roof girders, purlins and gutter beams are pinned by using vertical dowels at both ends. Lightweight roof panels, which rest on purlins, form the structural shape given in Fig. 2. Connections are fixed by grouting the holes around the dowels and/or threading and screwing the dowels after the installation of roof girders. During the investigation of design projects of 65 precast buildings, aforementioned parameters and their variations were determined. Building inventories have shown that structural properties of parallel frames that constitute the typical form of precast buildings were almost identical.

In Fig. 3, column dimensions and their variations are shown. It is seen that, majority of precast

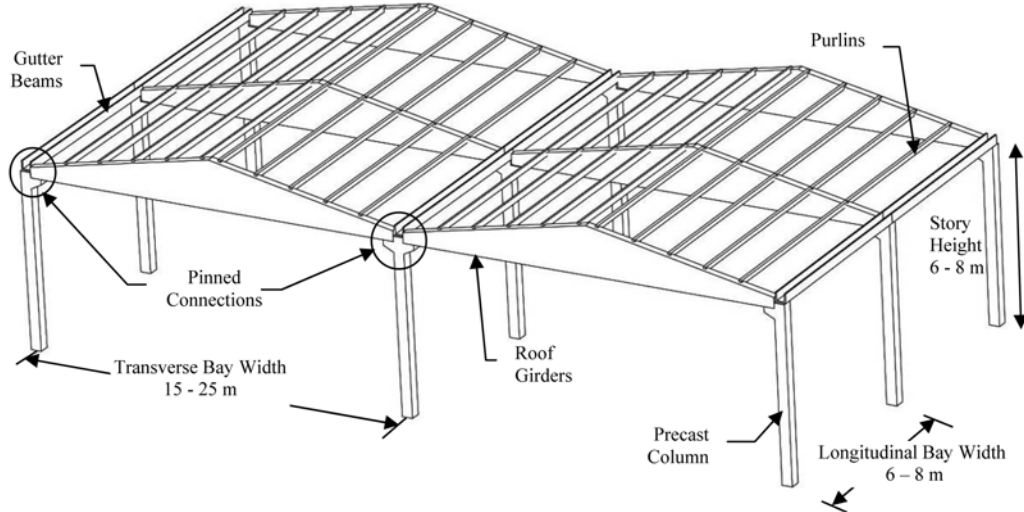


Fig. 2 Typical form of precast building which represents the large portion of Turkish industrial building stock

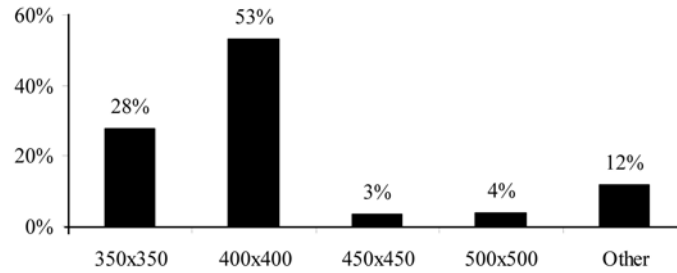


Fig. 3 Variation of typical column dimensions (mm) of investigated precast buildings

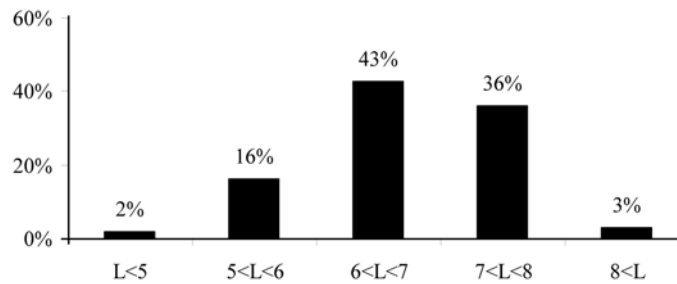


Fig. 4 Variation of building heights (m) according to precast building inventory

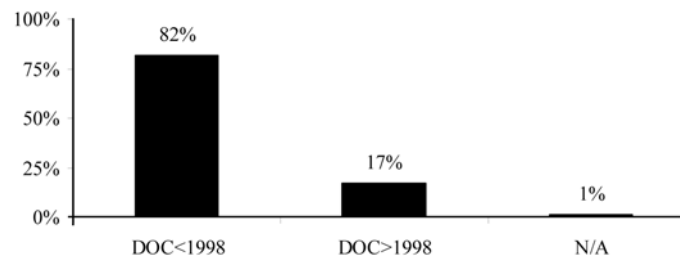


Fig. 5 Variation of date of constructions according to building inventory

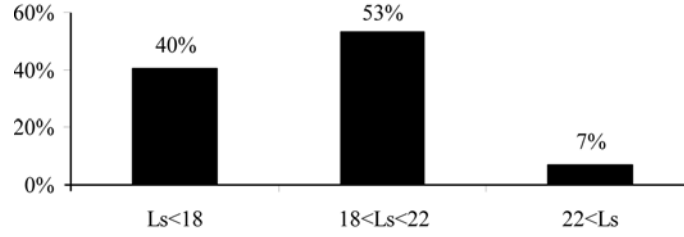


Fig. 6 Typical span lengths (m) of precast buildings

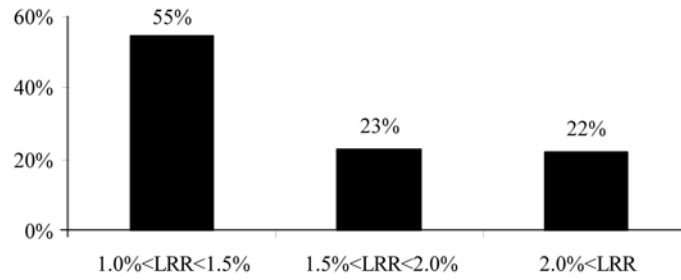


Fig. 7 Variation of longitudinal reinforcement ratios in precast columns

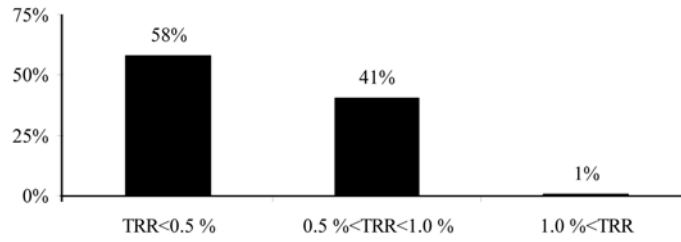


Fig. 8 Variation of volumetric transverse reinforcement ratios in columns

columns were constructed by using square members with 350 and 400 mm dimensions. Fig. 4, on the other hand, shows that about 80% of column heights are in between 6 and 8 m. Variation of dimensions and heights of columns verifies the slenderness of investigated precast building stock as being emphasized in previous studies. It should be reminded that majority of these slender buildings were constructed before the TEC-1998 regulations. In Fig. 5 distribution of construction dates of investigated buildings are given. Relatively smaller column dimensions which constitute the majority of inventory can be explained by former code rules that permit the use of lower seismic design forces without checking the displacements.

Fig. 6 shows that transverse bay widths of buildings vary between 18 and 22 m. These dimensions and common construction practice based on lightweight roof panels or cladding systems imply that the axial load levels in columns and hence the seismic weights are relatively small. Project based investigations have shown that S420 grade steel (Hot rolled ribbed reinforcement with $f_{yk} = 420$ MPa) was used in all precast columns and longitudinal reinforcement ratios are generally in between 1% and 1.5% (Fig. 7). In Turkish seismic design codes minimum and maximum longitudinal reinforcement ratios of columns are bounded by 1% and 4% respectively. Distribution of longitudinal reinforcement ratios shows that the design of precast columns is governed generally

by minimum requirements since the seismic forces considered in former designs are small. This situation is also valid for latter designs based on greater seismic forces which are calculated according to TEC-1998 definitions. But in this case design is generally governed by relative displacements that necessitate larger column dimensions as emphasized by Ersoy *et al.* (2000).

Concrete compressive strengths according to design projects varies between 25 and 35 MPa which can be thought to attain due to quality controlled manufacturing and curing process. Another important situation determined during the inventory study is about the transverse reinforcement content of columns. In Fig. 8, it can be clearly seen that transverse reinforcement ratios in the majority of precast columns are less than 0.5%. Former seismic design code (TEC-1975), defines the minimum transverse reinforcement ratio by Eq. (1). On the other hand, TEC-1998 and TEC-2007 defines the area of transverse reinforcement in each direction by the maximum of Eq. (2) or Eq. (3). In other words, both former and latter codes necessitate that the minimum required transverse reinforcement ratio for columns should be around 1%. Therefore, insufficient confinement level in inventory buildings can be explained neither old nor new code regulations. This situation emphasizes that, not only strength and stiffness but also ductility of existing precast structures should also be examined.

$$\rho_t = 0.12 \frac{f_{ck}}{f_{ywk}} \geq 1\% \quad (1)$$

$$A_{st} \geq 0.30 s b_k \left[\left(\frac{A_c}{A_{ck}} \right) - 1 \right] \left(\frac{f_{ck}}{f_{ywk}} \right) \quad (2)$$

$$A_{st} \geq 0.75 s b_k \left(\frac{f_{ck}}{f_{ywk}} \right) \quad (3)$$

Consequently, overall evaluation of building inventories have shown that structural properties determined from site investigations after the recent earthquakes (Atakoy 2000, Saatcioglu *et al.* 2001, Sezen and Whittaker 2006) and building inventories obtained from DOIZ are compatible with each other. Observations have also shown that structural configuration of all buildings in the inventory was similar with the building form considered in this study and sketched in Fig. 2. On the other hand, there can be precast buildings having different structural properties, member dimensions, connection details and architectural forms which are not compatible with the inventories. Therefore, it should be reminded that, comments and conclusions given in this study does not valid for these incompatible buildings which are thought to represent smaller portion of Turkish precast industrial building stock.

3. Analytical fragility curves for precast industrial buildings

Fragility curves are useful tools for evaluating the probability of structural damage due to earthquakes as a function of ground motion indices. They can be expressed as a conditional probability equation (Eq. (4)).

$$\Pr = P[R \geq r | I] \quad (4)$$

In this equation, R represents structural response, while r represents the minimum value of the

structural response for a given damage level. I is the ground motion parameter used as a random variable to estimate the probability of exceeding the selected damage levels during structural response.

There are many studies about fragility analysis in the literature for different classes of structures such as RC, masonry and steel buildings, bridges, etc. For any type of structure, structural analysis method, ground motion parameter, damage parameter and concerned damage levels affect the shape of fragility curves. Some typical examples and applications of fragility analysis from the literature are summarized as follows.

Karimi and Bakhshi (2006) proposed fragility curves for masonry buildings. They used Cumulative Absolute Velocity (CAV) as a ground motion parameter and Park-Ang (1985) model as a damage parameter. Monte-Carlo Simulation Method (Rubinstein 1989) was used to consider the uncertainty in structural parameters.

Karim and Yamazaki (2001) performed fragility analysis for bridges by selecting Park-Ang model as a damage parameter and PGA and PGV as ground motion parameters. They used nonlinear dynamic analysis for seismic demand calculation. In that study, lognormal distribution parameters were obtained by using least squares method.

Shinozuka *et al.* (2000a) used both nonlinear time history and nonlinear static analysis to construct fragility curves for bridges. In their study, section ductility demand was selected as damage parameter and PGA was used as ground motion parameter. Lognormal distribution parameters were obtained by maximum likelihood method. In another study statistical analysis of empirical and analytical fragility curves proposed for bridges were compared by Shinozuka *et al.* (2000b). In that study, damage data was gathered after Kobe earthquake for empirical curves, while nonlinear time history analysis was used for analytical curves. Lognormal distribution parameters were estimated by using maximum likelihood method.

Erberik and Elnashai (2004) selected drift ratio as damage parameter to construct fragility curves for mid-rise buildings having flat-slab systems. In that study spectral displacement (S_d) was used as ground motion parameter.

Kircil and Polat (2006) proposed fragility curves for mid-rise RC buildings in Istanbul, Turkey. They used drift ratio as a damage parameter and S_a , S_d and PGA as ground motion parameters. Akkar *et al.* (2005b) also proposed fragility curves for low-rise and mid-rise RC buildings in Turkey. The capacity of buildings was obtained by evaluating the existing building data. Drift ratio was selected as a damage parameter and PGV was selected as a ground motion parameter. Response parameters were obtained by using nonlinear time history analysis. Erberik (2007) and Ay *et al.* (2006) proposed another fragility curves for RC buildings in Turkey, depending on lognormally distributed PGV.

It can be said that residential buildings and bridges are the main concern of previous seismic fragility studies. But in this study, pin connected precast structures which represent the major portion of Turkish industrial building stock were considered. The other diversity applied in this study is about the definition of damage parameter. While, in many studies, damage parameter was defined in terms of ductility, drift ratio or damage indices, in this study it was directly calculated by using material strain limits. PGV was selected as ground motion parameter as being used in many previous studies. During the construction of fragility curves, calculation steps used by Kayhan (2008) were followed. The method applied for the fragility analysis of precast industrial buildings are listed and summarized as follows:

1. Prepare building inventories by investigating the design projects of 65 precast industrial buildings.
2. Construct the structural models that represent the precast building stock and obtain capacity curves.
3. Define the strain based damage levels on capacity curves.
4. Calculate the effective period and strength ratio in order get SDOF representation of analysis models.
5. Select the ground motion records and classify them by considering PGV values.
6. Perform nonlinear time history analysis and obtain displacement demands.
7. Make a damage assessment by comparing the damage limits and displacement demands for each strong motion record and building model.
8. Obtain the exceedence ratios of each damage level according to PGV intervals.
9. Estimate the parameters of lognormal distribution for each damage level with respect to PGV.
10. Construct and compare the fragility curves which reflect the variations in seismic risk due to different structural properties.

3.1 Representation of precast building stock by using analysis models

Building inventories used in this study and investigations performed after recent earthquakes give an idea about the building properties and their variations. In order to investigate the seismic behavior of precast buildings, analysis models which represent the structural properties of existing buildings were prepared. For this purpose, parameters that affect the strength, stiffness and ductility response of buildings were reflected by changing the cross sectional column dimensions (350 and 450 mm), transverse ($\rho_t = 0.4\%$, 0.7% and 1.0%) and longitudinal reinforcement ratios ($\rho_l = 1.0\%$ and 2.0%). By this way, twelve structural analysis models which are compatible with the building inventories and previous works were constructed. Three dimensional representation of precast model

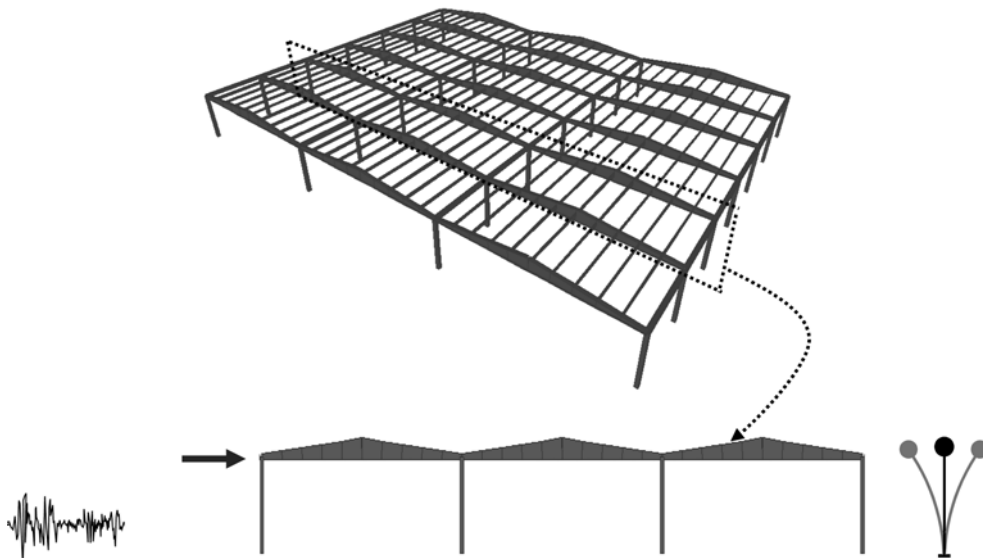
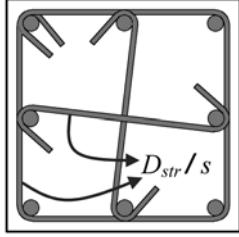


Fig. 9 Typical representation of precast building model and direction of loading considered

Table 1 Typical representation of column models and corresponding structural parameters

Typical Representation of Column Section	Model Names	$B \times H$	L	s	ρ_l	ρ_t
		mm	m	mm	%	%
 $f_{ck} = 30 \text{ MPa}$ $f_{yk} = f_{ywk} = 420 \text{ MPa}$ $D_{str} = 8 \text{ mm}$	B350-T1.0-L1	350×350	7	95	1%	1%
	B350-T1.0-L2	350×350	7	95	2%	1%
	B450-T1.0-L1	450×450	7	72	1%	1%
	B450-T1.0-L2	450×450	7	72	2%	1%
	B350-T0.7-L1	350×350	7	135	1%	0.7%
	B350-T0.7-L2	350×350	7	135	2%	0.7%
	B450-T0.7-L1	450×450	7	103	1%	0.7%
	B450-T0.7-L2	450×450	7	103	2%	0.7%
	B350-T0.4-L1	350×350	7	235	1%	0.4%
	B350-T0.4-L2	350×350	7	235	2%	0.4%
	B450-T0.4-L1	450×450	7	177	1%	0.4%
	B450-T0.4-L2	450×450	7	177	2%	0.4%

is given in Fig. 9. Considering the simplicity caused by pinned connections at roof level (Fig. 2), analytical studies were carried out by using two dimensional frame models which are loaded in the transverse direction. Names, notations and corresponding structural properties of analysis models are given in Table 1.

While preparing the analysis models, transverse and longitudinal bay numbers and widths, material strengths, roof loads etc. were considered as constant. Bay widths in transverse and longitudinal directions were taken as 20 m and 7.5 m. respectively. Compressive strength of concrete was taken as 30 MPa by considering quality controlled manufacturing process. Yield strength of longitudinal and transverse reinforcement bars were taken as 420 MPa and diameter of stirrups was assumed as 8 mm. Longitudinal reinforcement ratio of columns were arranged by changing the bar diameters. Transverse reinforcement ratio, on the other hand, was changed by using same stirrup diameter with various spacing as shown in Table 1.

Capacity curve of each precast building was obtained by first calculating force and displacement capacities of columns and then combining these individual responses. While calculating base shear capacity of precast system, it was assumed that seismic forces are acting at roof level (Fig. 9). Considering the cantilever behavior of columns, moment and shear capacity of members and then base shear capacity of building was obtained.

Non-linear behavior of precast system was modeled by using lumped-plasticity approach with nonlinear hinges placed at the base of columns. Curvature response beyond the elastic limit at plastic hinge regions was calculated by using moment-curvature analyses and curvature profile of each column was obtained. Representation of building model, assigned column sections, location of plastic hinges and typical moment curvature response at these hinge regions are shown schematically on Fig. 10. Moment-curvature analysis of column sections was performed by using spreadsheet software offered by Ersoy and Ozcebe (2001). In this software, confined and unconfined concrete behaviors of section fibers are represented by Modified Kent-Park Method (Park *et al.* 1982).

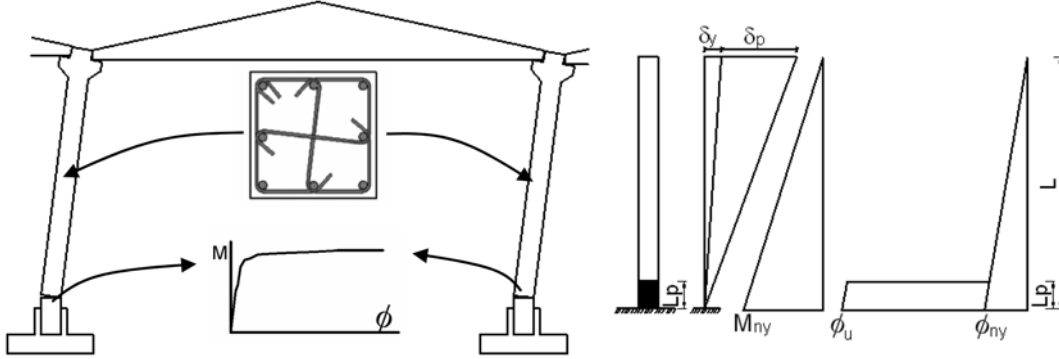


Fig. 10 Schematic representation of cantilever action and assumed curvature profile in precast columns

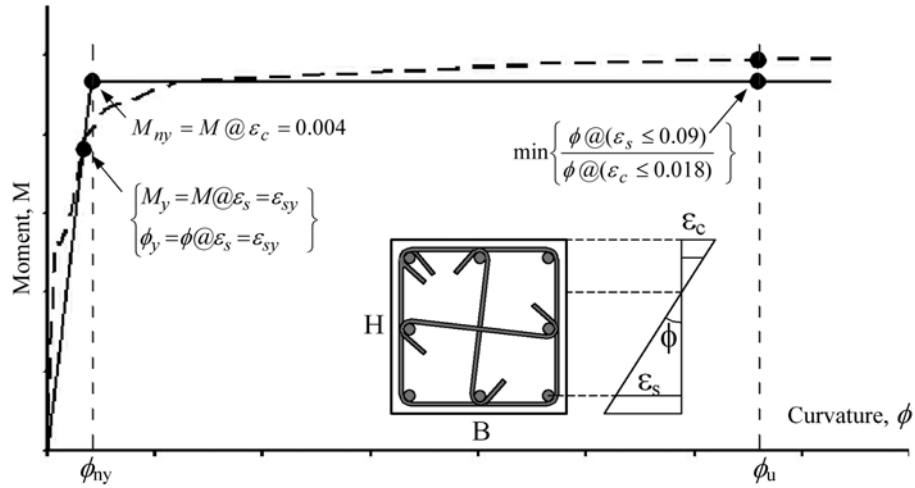


Fig. 11 Strain based limit state definitions and bilinear representation of moment curvature response

Detailed presentation of moment-curvature response of precast column section is given in Fig. 11. While determining nominal moment capacity of columns (M_{ny}), moment value at concrete strain of 0.004 was considered. Shear force (v_i) corresponding to this flexural capacity was then computed by using Eq. (5). Nominal yield curvature, on the other hand, was calculated by using the method sketched on Fig. 11. Numerical representation of this method is also given in Eq. (6).

$$v_{t_i} = \frac{M_{ny_i}}{L_i} \quad (5)$$

$$\phi_{ny_i} = \frac{M_{ny_i}}{M_{y_i}} \phi_{y_i} \quad (6)$$

For the calculation of ultimate curvature capacity of section, strain based limits were used. The ultimate compressive strain expression defined by Priestley *et al.* (1996) is given in Eq. (7). It can be clearly seen that, ultimate strain capacity of analysis models considered in this study can only be affected by transverse reinforcement ratio since the other parameters related with the material

properties are constant. In order to make compatible definition with the current Turkish Earthquake Code (TEC-2007), ultimate concrete strain was limited with 0.018. Ultimate tensile strain of longitudinal reinforcement was taken as 0.09 which was specified in some studies as ultimate strain limit for steel (Kowalsky 1997). It can be thought that this strain level corresponds to 75% of fracture strain of 0.12 for S420 grade steel.

$$\varepsilon_{cu} = 0.004 + \frac{1.4\rho_t f_{ywk} \varepsilon_{su}}{f_{cc}} \leq 0.018 \quad (7)$$

After the determination of yield and ultimate curvatures, plastic displacement capacity of precast columns was calculated by using Eq. (8). Although there are a lot of studies about the length of plastic hinge region, in this study definitions made by Park and Paulay (1975) and Fischinger *et al.* (2008) were considered and plastic hinge length (L_p) was taken as half of the section height. During the calculations, shear deformations were neglected by considering the slenderness of these structures.

$$\delta_{pi} = (\phi_{ui} - \phi_{nyi}) L_p \left(L - \frac{L_p}{2} \right) \quad (8)$$

Capacity curve of each precast building which is shown schematically in Fig. 12 was constructed by considering and combining elastic and plastic parts individually. Elastic part of capacity curve which is defined by total base shear (V_t) and yield displacement of structure (Δ_y) is calculated by using Eq. (9) and Eq. (10). During the calculations, effective stiffness of column sections was represented by 35% of gross stiffness ($I_{eff} = 0.35I_g$) regarding the low axial load ratios and experimental and theoretical studies from the literature (Elwood and Eberhard 2006, Hachem *et al.* 2003). Plastic displacement capacity of building (Δ_p), on the other hand, was determined by selecting the minimum of column plastic displacement capacities which were calculated according to Eq. (8). Definition of plastic displacement capacity of precast building is expressed by Eq. (11).

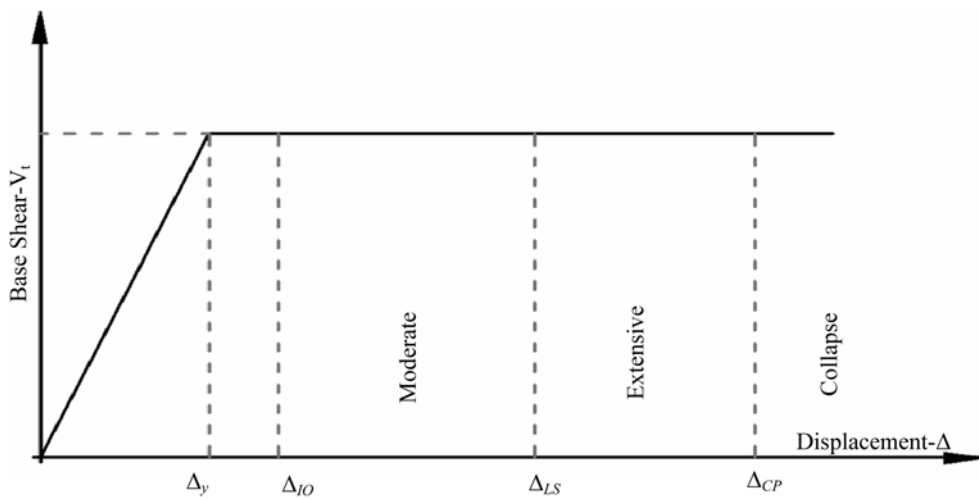


Fig. 12 Combination of column responses to represent overall capacity curve of structure

$$V_t = \sum_{i=1}^n v_{t_i} \quad (9)$$

$$\Delta_y = \frac{V_t \cdot L^3}{3 \cdot \sum E \cdot I_{eff}} \quad (10)$$

$$\Delta_p = \min(\delta_{p_i}) \quad (11)$$

Both Figs. 11 and 12 imply that structural damage increases with increasing plastic curvatures, strain levels and displacements. In order to classify building damage, immediate occupancy, life safety and collapse prevention limits corresponding to 10%, 60% and 90% of plastic displacement capacity (Δ_p), were taken into account in order to specify moderate, extensive and collapse cases respectively. Displacements beyond the collapse prevention limit were considered as the indicator of collapse. Detailed expression of this damage classification process is expressed by using Eqs. (12) to (14). Although all damage states from slight to collapse are shown on Fig. 12, extensive and collapse cases were mainly considered in this study since these damages can be associated with the partial or total collapse.

$$\Delta_{IO} = \Delta_y + 0.10 \cdot \Delta_p \quad (12)$$

$$\Delta_{LS} = \Delta_y + 0.60 \cdot \Delta_p \quad (13)$$

$$\Delta_{CP} = \Delta_y + 0.90 \cdot \Delta_p \quad (14)$$

The abovementioned method applied for the construction of typical capacity curve of B350-T0.7-L2 building is summarized by using Table 2 and 3. Although, structural properties of columns in each individual analysis model are identical, moment and curvature capacities corresponding to inner and outer columns can be slightly different due to different axial loads. In Table 2, moment, shear and curvature response of inner and outer columns are given. In Table 3, lateral strength ratio, vibration period and displacement response of typical frame composed of those inner and outer columns are shown.

Table 2 Moment-Curvature analysis results for columns

Columns	M_{ny}	v_t	ϕ_{ny}	ϕ_u
	kNm	kN	rad/m	rad/m
Outer	157.63	22.52	0.0122	0.238
Inner	170.18	24.31	0.0124	0.183

Table 3 Capacity curve parameters for frame B350-T0.7-L2

Frame	V_t/W	Δ_y	Δ_{IO}	Δ_{LS}	Δ_{CP}	T
	%	mm	mm	mm	mm	s
B350-T0.7-L2	9.6	191.14	211.82	315.24	377.29	2.83

Table 4 Mean and median values of PGV groups (cm/s)

Group	Mean	Median
1	21.97	21.93
2	27.76	27.92
3	32.50	32.72
4	37.66	37.61
5	42.35	42.11
6	47.67	47.77
7	52.21	51.99
8	57.27	57.47
9	62.32	62.45
10	67.58	67.50
11	72.55	72.48
12	77.28	77.48

3.2 Input ground motions and dynamic analysis

Precast frames represented by nonlinear SDOF models (as summarized in Table 3) were analyzed by using strong ground motion records and displacement demands were determined. In order to include a wider range of variation of input ground motions, 360 records from 28 different earthquakes were used for nonlinear dynamic analysis. Records were taken from PEER Strong Motion Database. Magnitudes of the selected earthquakes range from 5.4 to 7.7. For almost all the records the closest distance to the fault is smaller than 30 km.

Previous studies have shown that PGV well correlates with maximum displacement demand with respect to many other ground motion parameters (Akkar *et al.* 2000a, Akkar *et al.* 2000b). Therefore, in this study, PGV was considered as a ground motion parameter while constructing the fragility curves. Ground motions which have PGV values between 20 and 80 cm/s were classified into 12 sub-groups by considering 5 cm/s intervals. While selecting the records, it was intended to use of uniformly distributed velocities in order to prevent the accumulation of dynamic analysis results. Therefore 30 records were selected in each of 12 PGV sub group. During the analysis, 288 records were used in their original formats. In order to obtain necessary amount of data especially for higher PGV values, 72 records were scaled. Maximum factor used for the scaling of ground motions is 1.54. Table 4 shows mean and median values of PGV groups. It can be seen that, mean and median values of each PGV group are very close to each other. While obtaining fragility curves, each PGV group is represented by mean values.

For nonlinear dynamic analysis, Sap2000 (2004) program was used. Average Acceleration Method (Newmark 1959) was selected for the numerical integration. Hysteretic response was represented by ideal elasto-plastic behavior. In seismic demand calculations, viscous damping ratios of 2% to 7% were recommended for various type of reinforced concrete structures (Chmielewski *et al.* 1999). In this study, previous investigations for precast buildings (Priestley *et al.* 1999, Englekirk 2003) and cantilever type SDOF structures (Priestley *et al.* 1996, Priestley *et al.* 2007) were considered while deciding the viscous damping ratio, since the analysis models can be related with both of them. As a result of this investigation, viscous damping ratio was taken as 5% during the nonlinear time history analysis. It should be noted that definition of seismic demand in many building codes are also compatible with this assumption.

Table 5 Fragility curve parameters for precast industrial building models

Models	Mod. (>IO)		Ext. (>LS)		Col. (>CP)	
	λ	ζ	λ	ζ	λ	ζ
B350-T1.0-L1	3.573	0.352	4.041	0.472	4.330	0.494
B350-T1.0-L2	3.741	0.352	4.156	0.434	4.399	0.387
B450-T1.0-L1	3.705	0.378	4.439	0.290	4.540	0.207
B450-T1.0-L2	3.961	0.380	4.816	0.464	4.962	0.441
B350-T0.7-L1	3.535	0.370	3.913	0.369	4.199	0.511
B350-T0.7-L2	3.716	0.355	4.046	0.363	4.271	0.398
B450-T0.7-L1	3.708	0.384	4.465	0.305	4.540	0.207
B450-T0.7-L2	3.926	0.385	4.567	0.353	4.831	0.386
B350-T0.4-L1	3.457	0.395	3.767	0.346	3.879	0.385
B350-T0.4-L2	3.686	0.346	3.882	0.322	3.986	0.347
B450-T0.4-L1	3.553	0.432	4.118	0.278	4.379	0.269
B450-T0.4-L2	3.876	0.393	4.224	0.275	4.356	0.163

3.3 Construction of analytical fragility curves

Utilizing the results of nonlinear dynamic analysis, fragility curves for each frame were constructed. Maximum displacement demand obtained after the analysis of each frame was compared with the limit displacement of damage levels. By this way, exceedence numbers and exceedence ratios for each PGV group and each damage level were obtained. Fragility curves were then constructed by using these exceedence ratios and by assuming two-parameter lognormal distribution. Parameters of lognormal distribution, mean (λ) and standard deviation (ζ), were estimated by using least squares method. Eq. (15) expresses the cumulative probability of exceeding the selected damage level.

$$\text{Pr} = \Phi \left[\frac{\ln Y - \lambda}{\zeta} \right] \quad (15)$$

In Eq. (15), Φ represents standard cumulative normal distribution function and Y represents ground motion parameter (in this study, PGV). Table 5 shows lognormal distribution parameters of moderate, extensive and collapse cases.

4. Effect of structural parameters on fragility curves

Analytical models prepared by considering the inventory represents the different strength, stiffness and ductility groups of existing precast buildings. Results of inventory study based on 65 precast buildings imply that majority of existing buildings are composed of columns which constitutes lower bounds of properties such as smaller dimensions and/or lower longitudinal and transverse reinforcement ratios. Therefore, analysis models prepared especially by using 350 mm section dimensions and 0.4% of transverse reinforcement ratio are used in order to represent existing precast building stock. On the other hand, superior buildings modeled by using 450 mm column dimensions, 1% transverse reinforcement ratios and 2% longitudinal reinforcement ratios are used in

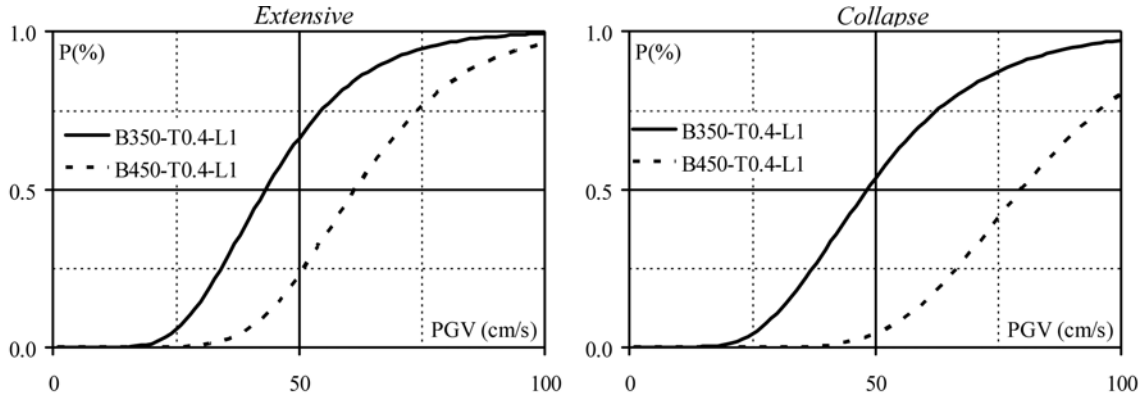


Fig. 13 Efficiency of stiffness on the fragility response of B350-T0.4-L1 and B450-T0.4-L1 buildings

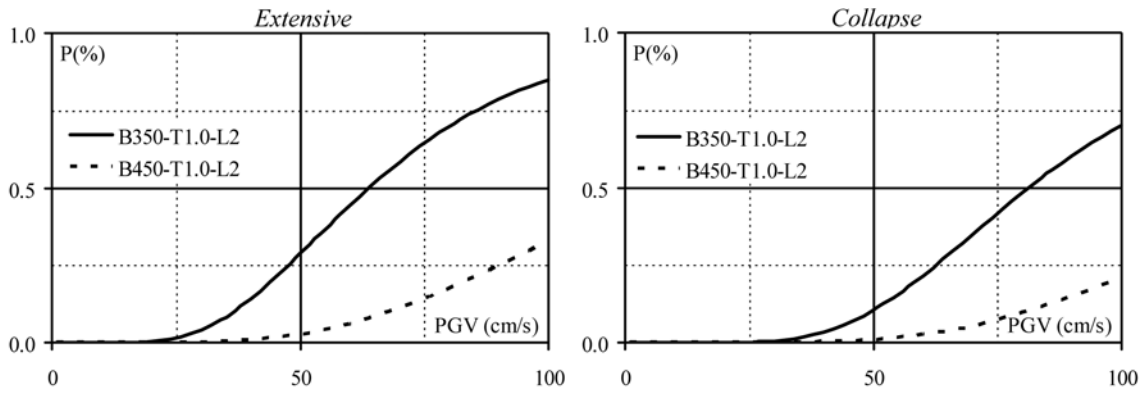


Fig. 14 Efficiency of stiffness on the fragility response of B350-T1.0-L2 and B450-T1.0-L2 buildings

order to represent relatively new, strong, stiff and ductile buildings. In this section, first the efficiency of stiffness, strength and ductility properties of existing, new and moderate buildings were investigated and then PGV based failure probabilities of existing precast buildings were discussed.

In Fig. 13 fragility curves of B350-T04-L1 and B450-T04-L1 models are given in order to investigate the efficiency of stiffness by comparing the damage probabilities of extensive damage and collapse cases. Remarkable differences in damage probabilities for both cases can be seen in this figure. Fig. 14 also shows that, same situation is valid for similar buildings that include higher amount of transverse and longitudinal reinforcement content (B350-T1.0-L2 and B450-T1.0-L2). Evaluating the fragility curves given in Figs. 13 and 14, it can be concluded that, the stiffness capacity of columns have considerable effect on the damage and failure probabilities of precast buildings.

The effect of ductility capacity on the fragility response of building models are represented in Fig. 15 and 16. It can be clearly seen that considerably higher damage probabilities, for both extensive and collapse cases, are allocated by poorly confined buildings which have transverse reinforcement content of 0.4%. This situation shows the vulnerability of existing precast building stock composed by such kind of poorly confined buildings.

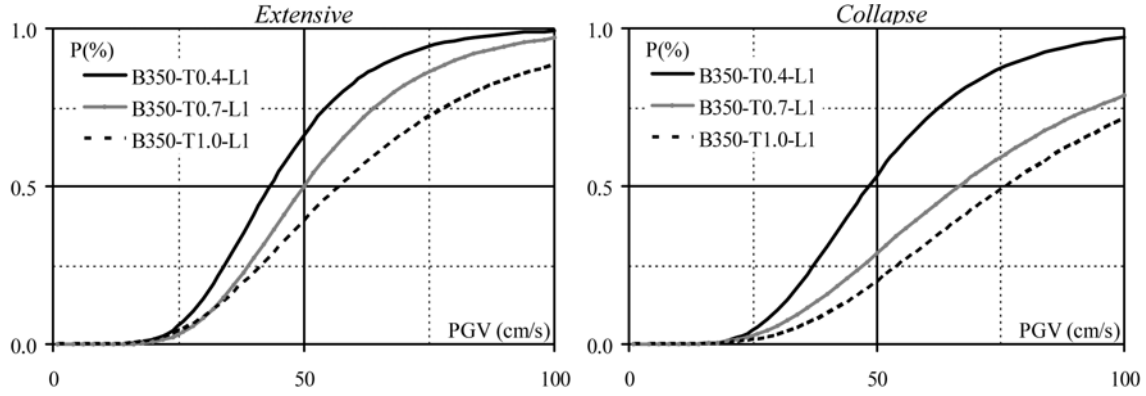


Fig. 15 Efficiency of ductility on the fragility response of slender building models

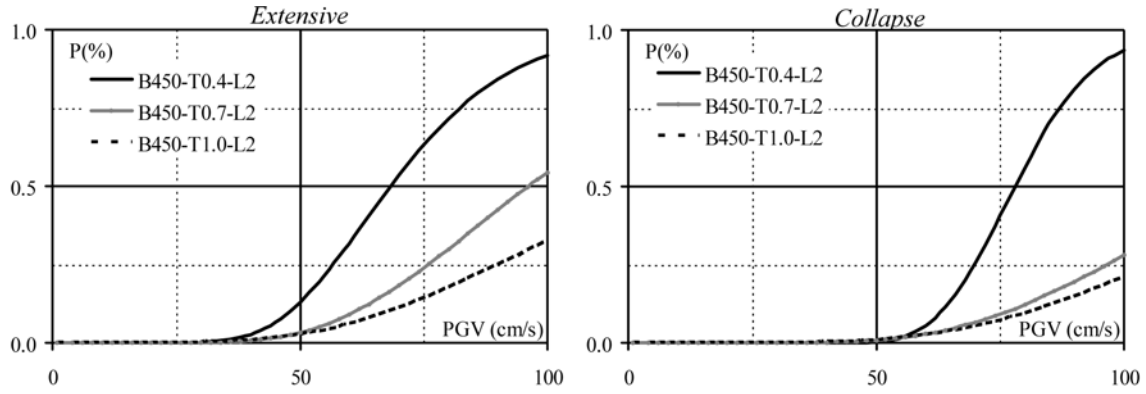


Fig. 16 Efficiency of ductility on the fragility response of stiffer and stronger building models

Efficiency of transverse reinforcement content in buildings which have stiffer (450×450 mm) and stronger ($\rho_l = 2\%$) columns is shown in Fig. 16. The observed shifts to the right side for each damage state and each transverse reinforcement ratio show that damage probabilities corresponding to identical seismic demand levels are decreasing. Fig. 16 also shows that extensive damage and collapse probabilities of poorly confined but stronger and stiffer buildings (B450-T0.4-L2) imply much more critical situation with respect to moderately and well confined buildings (B450-T0.7-L2 and B450-T1.0-L2). In other words, the efficiency of strength and stiffness characteristics of buildings can directly be affected by the confinement level of the columns.

Fig. 17 shows the fragility curves of both poorly and well confined slender buildings that have different strength capacities when collapse state is considered. Although failure probabilities corresponding to different confinement levels ($\rho_l = 0.4\%$ and 1.0%) are quite different from each other, no significant changes are detected due to strength variation caused by different longitudinal reinforcement content. This situation presented for slender columns is also valid for stiffer columns (450×450 mm) as shown in Fig. 18. Therefore, it can be said that strength capacity of precast buildings is not as effective as stiffness and ductility. In other words, damage probabilities beyond the excessive damage are especially controlled by stiffness and ductility rather than strength.

At this point it may need to review the code regulations came into force with TEC-1998 and

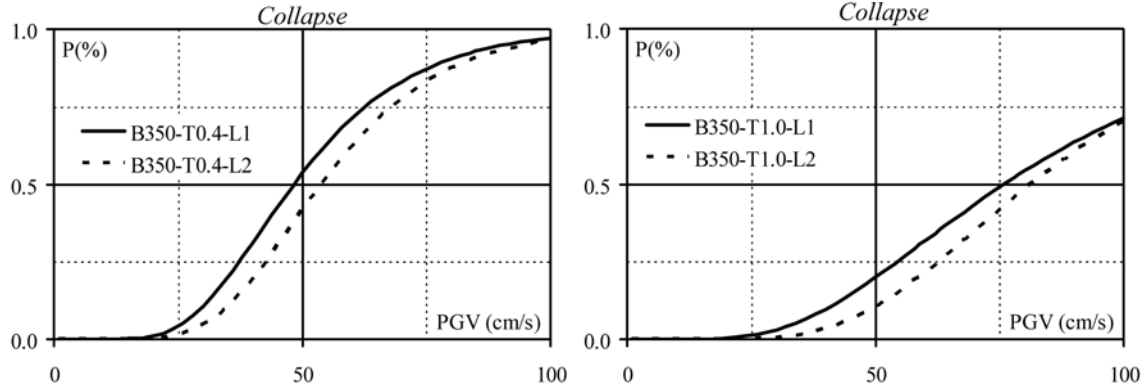


Fig. 17 Efficiency of strength on the fragility response of slender buildings for collapse case

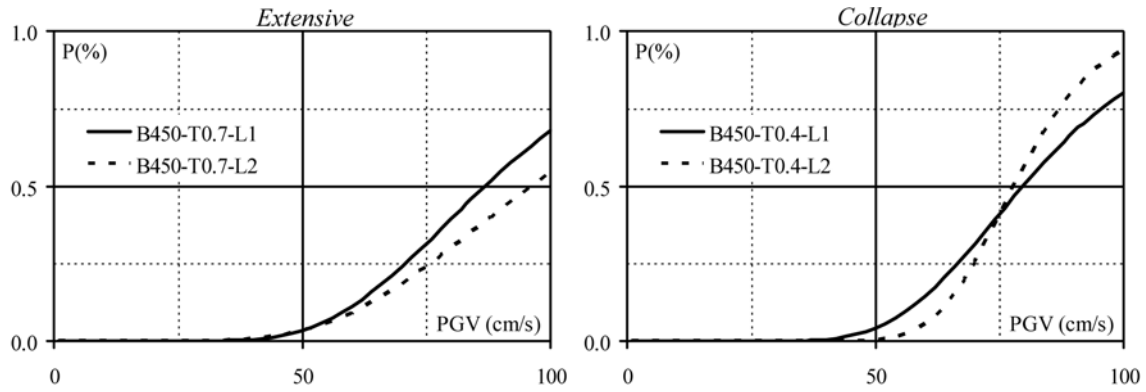


Fig. 18 Efficiency of strength on the fragility response of stiffer building models

TEC-2007. It should be noted that the majority of existing precast buildings in Turkey were constructed before 1998 (Fig. 5). In fact TEC-1998 rules for the design of precast buildings mainly include two distinct regulations. One of them was about force reduction factor (R) which is defined as 5. The other regulation was about the allowable elastic drift limit which is defined as 0.0035. In precast buildings, low axial loads and cantilever behavior of slender columns reduces the lateral stiffness while increasing the vibration period and hence the displacement demand of the system. Consequently, lateral force calculated for the design of precast columns necessarily become small. Therefore, in most cases allowable drift limits enforced by the TEC-1998 governs the design as being emphasized by Ersoy *et al.* (2000). The designs, on the other hand, controlled by drift limits necessitate stiffness rather than strength. As a result of this situation, reinforcement content of columns was generally determined by minimum requirements.

In 2007, current code was published (TEC-2007) and modification was made by decreasing the R factor from 5 to 3 in order to increase strength capacity considered in design. It should be noted that design strengths attained after this regulation are closer to Eurocode 8 ($R = 1.5$), UBC-1997 ($R = 2.2$) and FEMA-450 ($R = 2.5$) based designs. Besides the definition of seismic design forces, extent of lateral displacements was also changed in TEC-2007 by assigning the ultimate drift ratio of 2%. This definition is identical with the other drift limit definitions of Eurocode 8, UBC-1997 and FEMA 450 provisions. Elastic drift calculated by using ultimate drift ratio and the new R factor

($0.0067 = 0.02/R$) permits the use of larger allowable displacements for design. By this way, the abovementioned problem caused by inconsistency between strength and drift definitions of former code was thought to be resolved. As a result of these investigations it can be said that the designs based on TEC-2007 give reasonable and comparable results with respect to Eurocode 8 and UBC-1997 codes and FEMA-450 provisions.

On the other hand, the results of fragility analysis emphasize the efficiency of stiffness and ductility rather than strength. Confinement levels (Fig. 8) and construction dates of inventory buildings (Fig. 5) have shown that neither ductility nor stiffness requirements of both TEC-1998 and TEC-2007 codes (which were criticized above) could be satisfied in majority of existing precast buildings. Slenderness of these structures imply the need for more displacement capacity which is only achieved by ductility. Therefore, displacement capacity of precast buildings which is governed by ductility should be emphasized in the codes as well as strength and stiffness.

5. Damage estimation in existing precast buildings by using fragility curves

Considering the results of inventory study and former code rules, the term “existing precast buildings” was used in order to identify the buildings that have smaller column dimensions and inadequate confinement reinforcement. Therefore, while evaluating the damage probabilities of these buildings, fragility curves constructed for B350-T0.4-L1 model was used. As can be seen from Fig. 19, damage probabilities for each damage states increases with the increasing seismic demand. In order to make reasonable estimation of damage, PGV values between 40 and 70 cm/sec. were accepted as the indicator of destructive earthquakes. Peak velocities of many strong earthquakes between these values confirm this situation. Maximum velocities around 70 cm/sec determined from the records of different stations during Kocaeli Earthquake also verify the compatibility of this assumption. Fig. 19 shows that, collapse probabilities of existing buildings may change approximately from 25% to 75% between these PGV intervals. If extensive damage is accepted as the indicator of partial or total collapse, then these probabilities can be increased approximately 10%. Site investigation after Kocaeli Earthquake which represented by Ersoy *et al.* (2000) have shown that, in some industrial regions the ratio of totally or partially collapsed precast buildings reached up to 80%. This situation demonstrates the similarity between the upper limits of observed

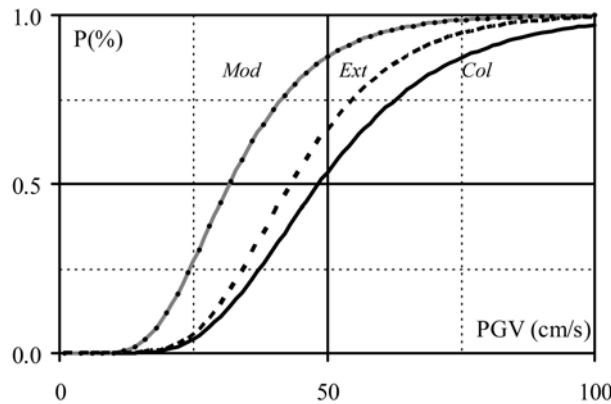


Fig. 19 Damage estimation in existing precast buildings by using fragility curves (B350-T0.4-L1)

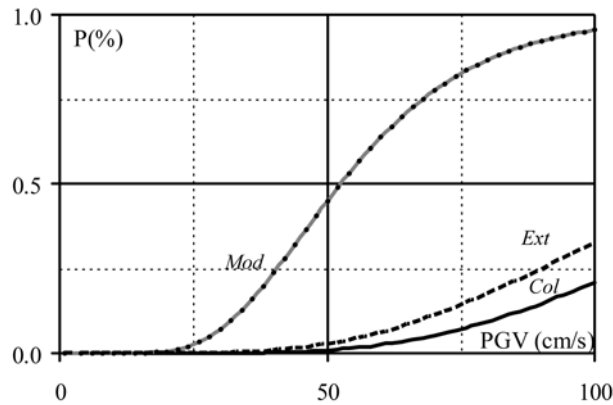


Fig. 20 Damage estimation in superior precast buildings by using fragility curves (B450-T1.0-L2)

and calculated collapse ratios. Fig. 19 also shows that great majority of existing precast buildings should be expected to exceed moderate damage state during strong earthquakes. Aforementioned study performed by Cruz *et al.* (2005) indicates the similar situation. According to that study, overall evaluation of the affected regions showed that economical losses were reported by around 60% of industrial facilities after Kocaeli and Duzce Earthquakes.

It can be thought that buildings modeled by using well confined, stiffer and stronger columns represent the seismic designs according to new codes and hence buildings constructed after 1998. On the other hand these buildings constitute the small portion of inventories. These superior buildings represented by an analysis model of B450-T1.0-L2. Damage estimation was also performed for this type of building as shown in Fig. 20. Considerable difference between the damage probabilities of new and old buildings can be observed by comparing Fig. 19 and 20. Seismic performance of new buildings designed according latter codes is much better with respect to old buildings.

6. Conclusions

Structural properties of existing precast buildings were determined by evaluating the design project of 65 precast buildings constructed in Denizli Organized Industrial Zone. The results of inventory study have shown that the majority of existing precast buildings are composed by slender and poorly confined buildings. It was also determined that majority of buildings were constructed before the publication of modern seismic design code of TEC-1998.

Analytical models of precast buildings were prepared by reflecting the results of inventory study and by considering the reported properties of buildings in recent earthquakes. Investigations performed by comparing the stiffness, strength and ductility capacities of building models have shown that the most effective parameters that govern the damage and collapse probabilities of precast buildings are stiffness and ductility. Similar failure probabilities corresponding to different strength levels show that strength capacity is not as effective as stiffness and ductility.

This situation shows that, displacement capacity of precast buildings which is governed by stiffness and ductility should be emphasized as well as strength capacity which is arranged by R factors.

Investigating the seismic performance of existing buildings showed that the results of fragility

analysis and damage and failure observations performed after Kocaeli and Duzce Earthquakes are compatible. On the other hand, fragility analysis of new buildings designed according to latter codes indicates considerably higher performance with respect to old ones.

Acknowledgements

The research reported in this paper was supported by Pamukkale University Research Fund under Project No. 2006MHF008. The authors wish to express their deep gratitude to Tanju Bestas who is the director of Denizli Organized Industrial Zone for providing the design projects of precast buildings and Turkish Precast Concrete Association for supporting the graduate studies about the precast structures. Thanks are also extended to graduate student M. Palanci who still contributes the ongoing studies about precast buildings.

References

- Adalier, K. and Aydingun, O. (2001), "Structural engineering aspects of the June 27, 1998 Adana-Ceyhan (Turkey) earthquake", *Eng. Struct.*, **23**(4), 343-355.
- Akkar, S. and Ozen, O. (2005), "Effect of peak ground velocity on deformation demands for SDOF systems", *Earthq. Eng. Struct. D.*, **34**, 1551-1571.
- Akkar, S., Sucuoglu, H. and Yakut, A. (2005), "Displacement-based fragility functions for low and mid-rise ordinary concrete buildings", *Earthq. Spectra*, **21**(4), 901-927.
- Arsilan, M.H., Korkmaz, H.H. and Gulay, F.G. (2005), "Damage and failure pattern of prefabricated structures after major earthquakes in Turkey and shortfalls of the Turkish earthquake code", *Eng. Fail. Anal.*, **13**, 537-557.
- Atakoy, H. (2000), "The August 17th Earthquake and the prefabricated structures built by the members of the prefabric union", *Concrete Prefabrication*, No:52-53 (in Turkish).
- Ay, B.Ö., Erberik, M.A. and Akkar, S. (2006), "Fragility based assessment of the structural deficiencies in Turkish RC frames structures", *First European Conference on Earthquake Engineering and Seismology*, Geneva, Switzerland.
- Chmielewski, T., Kratzig, W.B., Link, M., Meskouris, K. and Wunderlich, W. (1996), *Phenomena and Evaluation of Dynamic Structural Responses*, in *Dynamics of Civil Engineering Structures*, W.B. Kratzig and H.J. Niemann, (Eds.), A.A. Balkema, Rotterdam.
- Cruz, A.M. and Steinberg, L.J. (2005), "Industry preparedness for earthquakes and earthquake-triggered hazard accidents in the 1999 Kocaeli earthquake", *Earthq. Spectra*, **21**(2), 285-304.
- Elwood, K.J. and Eberhard, M.O. (2006), "Effective stiffness of reinforced concrete columns", *PEER Research Digest*, No. 2006-1.
- Englekirk R.E. (2003), *Seismic Design of Reinforced and Precast Concrete Buildings*, John Wiley & Sons, Hoboken, New Jersey.
- Erberik, M.A. (2007), "Fragility-based assessment of typical mid-rise and low-rise RC buildings in Turkey", *Eng. Struct.*, **30**, 1360-1374.
- Erberik, M.A. and Elnashai, A.S. (2004), "Fragility analysis of flat-slab structures", *Eng. Struct.*, **26**, 937-948.
- Ersay, U. and Özcebe, G. (2001), *Reinforced Concrete*, Evrim Publications, Istanbul. (in Turkish)
- Ersay, U., Özcebe, G. and Tankut, T. (2000), "Observed precast building damages in 1999 Marmara and Duzce earthquakes", *10th Prefabrication Symposium*, Istanbul. (in Turkish).
- Eurocode 8 (1998), "Design design provisions for earthquake resistance of structures", European Union, European Prestandarts, Brussel.
- Fischinger, M., Kramar M. and Isakovic T., (2008), "Cyclic response of slender RC columns typical of precast industrial buildings", *B. Earthq. Eng.*, **6**, 519-534.
- Hachem, M.M., Mahin, S.A. and Moehle, J.P. (2003), *Performance of Circular Reinforced Concrete Bridge*

- Columns under Bidirectional Earthquake Loading*, Pacific Earthquake Engineering Research Center, PEER Rep. No. 2003-06, University of California
- Karaesmen, E. (2001), *Prefabrication in Turkey: Facts and Figures*, Department of Civil Engineering, Middle East Technical University, Ankara, Turkey.
- Karim, K.R. and Yamazaki, F. (2001) "Effect of earthquake ground motions on fragility curves of highway bridge piers based on numerical simulation", *Earthq. Eng. Struct. D.*, **30**, 1839-1856.
- Karimi, K. and Bakhshi, A. (2006), "Development of fragility curves for unreinforced masonry buildings before and after upgrading using analytical method", *First European Conference on Earthquake Engineering and Seismology*, Geneva, Switzerland.
- Kayhan, A.H. (2008), *Damage and Economic Loss Estimation for Pin Connected Precast Buildings*, PhD Thesis, Pamukkale University, Denizli, November.
- Kirçil, M.S. and Polat, Z. (2006), "Fragility analysis of mid-rise RC frame buildings", *Eng. Struct.*, **28**(9), 1335-1345.
- Kowalsky, M.J. (1997), *Direct Displacement-Based Design: A Seismic Design Methodology and Its Application to Concrete Bridges*, PhD Dissertation, University of California, San Diego.
- Newmark, N.M. (1959), "A method of computation for structural dynamics", *J. Eng. Mech.*, ASCE, **85**, 67-94.
- Park, Y.J. and Ang, A.H. (1985), "Seismic damage analysis of reinforced concrete buildings", *J. Struct. Eng.*, ASCE, **111**(4), 740-757.
- Park, R. and Paulay, T. (1975), *Reinforced Concrete Structures*, John Wiley & Sons, New York.
- Park, R., Priestley, M.J.N. and Gill, W.D. (1982), "Ductility of square-confined concrete columns", *J. Struct. Div.*, ASCE, **108**(ST4), 929-950.
- PEER Strong Ground Motion Database, <http://peer.berkeley.edu/smcat/>
- Posada, M. and Wood, S.L. (2002), "Seismic performance of precast industrial buildings in Turkey", *7th National Conference on Earthquake Engineering (7NCEE)*, Boston.
- Priestley, M.J.N., Seible, F. and Calvi, G.M. (1996), *Seismic Design and Retrofit of Bridges*, John Wiley & Sons, New York.
- Priestley, M.J.N., Calvi, G.M. and Kowalsky, M.J. (2007), *Displacement Based Seismic Design of Structures*, IUSS Press, Pavia, Italy.
- Priestley, M.J.N., Sritharan, S., Conley, J.R. and Pampanin, S. (1999), "Preliminary results and conclusions from the PRESS five-story precast concrete test building", *PCI J*, **44**(6), 42-67.
- Rubinstein, R.Y. (1989), *Simulation and the Monte Carlo Method*, John Wiley & Sons, New York.
- Saatcioglu, M., Mitchell, D., Tinawi, R., Gardner, N.J., Gillies, A.G., Ghobarah, A., Anderson, D.L. and Lau, D. (2001), "The August 17, 1999 Kocaeli (Turkey) earthquake-damage to structures". *Can. J. Civil Eng.*, **28**(8), 715-773.
- SAP2000 (2004), *Integrated Software for Structural Analysis & Design*, Computers and Structures Inc., California, USA.
- Sezen, H., Elwood, K.J., Whittaker, A.S., Mosalam, K.M., Wallace, J.W. and Stanton, J.F. (2000), *Structural Engineering Reconnaissance of the August 17, 1999 Kocaeli (Izmit), Turkey Earthquake*, PEER Rep. No.2000-09, Pacific Earthquake Engineering Research Center, University of California.
- Sezen, H. and Whittaker, A.S. (2006), "Seismic performance of industrial facilities affected by the 1999 Turkey earthquake", *J. Perform. Constr. Fac.*, **20**(1), 28-36.
- Shinozuka, M., Feng, M.Q., Kim, H.K. and Kim, S.H. (2000), "Nonlinear static procedure for fragility curve development", *J. Eng. Mech.*, ASCE, **126**(12), 1287-1295.
- Shinozuka, M., Feng, M.Q., Lee, J. and Naganuma T. (2000), "Statistical analysis of fragility curves", *J. Eng. Mech.*, ASCE, **126**(12), 1224-1231.
- TEC-1975, Turkish Earthquake Code (1975), Specifications for structures to be built in disaster areas, Ministry of Public Works and Settlement, Ankara, Turkey.
- TEC-1998, Turkish Earthquake Code (1998), Specifications for structures to be built in disaster areas, Ministry of Public Works and Settlement, Ankara, Turkey.
- TEC-2007, Turkish Earthquake Code (2007), Specifications for structures to be built in seismic areas, Ministry of Public Works and Settlement, Ankara, Turkey.
- Tezcan, S.S. and Colakoglu, H.K. (2003), "Weak Points Of The TEC-98 Precast Building Code Provisions",

Fifth National Conference on Earthquake Engineering, Istanbul, Turkey.
 Uniform Building Code (1997), *International Conference of Building Officials*, Whittier, California.
 Zorbozan M., Barka G. ve Sarifakioglu F. (1998), “Observed precast building damages in ceyhan earthquake, reasons and solutions”, *Concrete Prefabrication*, **48**, 20-24 (in Turkish).

Notation

A_c	: Cross sectional area of column section
A_{ck}	: Cross-sectional area confined by transverse reinforcement
A_{st}	: Cross-sectional area of transverse reinforcing bars
b_k	: Distance between the centers of outermost transverse bars
B	: Width of column cross section
D_{str}	: Stirrup diameter
f_{ck}	: Concrete compressive strength
f_{cc}	: Confined concrete compressive strength
f_{yw}	: Tensile strength of transverse reinforcement
H	: Height of column cross section
L	: Column height
L_p	: Plastic hinge length
M_{ny}	: Nominal yield moment of precast columns
M_y	: Yield moment of precast columns
s	: Spacing between stirrups
v_t	: Column shear strength
V_t	: Base shear capacity of precast building
ε_s	: Steel tensile strain
ε_{su}	: Ultimate tensile strain of steel
ε_c	: Concrete compression strain
ε_{cu}	: Ultimate compression strain for concrete
ρ_l	: Longitudinal reinforcement ratio of columns
ρ_t	: Volumetric transverse reinforcement ratio of columns
δ_p	: Plastic displacement capacity of columns
ϕ_{ny}	: Nominal yield curvature of column section
ϕ_u	: Ultimate curvature capacity of column section
Δ_y	: Elastic displacement of precast building
Δ_p	: Plastic displacement capacity of precast building
Δ_{IO}	: Plastic displacement corresponding to Immediate Occupancy damage limit
Δ_{LS}	: Plastic displacement corresponding to Life Safety damage limit
Δ_{CP}	: Plastic displacement corresponding to Collapse Prevention damage limit
λ	: Mean value of the distribution
ζ	: Standard deviation of the distribution

Abbreviations

DOC	: Date of construction
DOIZ	: Denizli organized industrial zone
LRR	: Longitudinal reinforcement ratio
PGA	: Peak ground acceleration
PGV	: Peak ground velocity
TRR	: Transverse reinforcement ratio
UBC	: Uniform Building Code